

Proton-induced magnetic order in carbon: SQUID measurements¹

J. Barzola-Quiquia, S. Petriconi, P. Esquinazi*, M. Rothermel, D. Spemann, A. Setzer,
T. Butz

Institut für Experimentelle Physik II, Universität Leipzig, Linnéstrasse 5, D-04103 Leipzig, Germany

Abstract

In this work we have studied systematically the changes in the magnetic behavior of highly oriented pyrolytic graphite (HOPG) samples after proton irradiation in the MeV energy range. Superconducting quantum interferometer device (SQUID) results obtained from samples with thousands of localized spots of micrometer size as well on samples irradiated with a broad beam confirm previously reported results. Both, the para- and ferromagnetic contributions depend strongly on the irradiation details. The results indicate that the magnetic moment at saturation of spots of micrometer size is of the order of 10^{-10} emu.

Key words: carbon, irradiation effects, magnetic order

PACS: 75.50.Dd, 75.70.Rf, 61.72.Ss

1. Introduction

Magnetic order at room temperature in metal-free carbon-based structures remains one of the exciting issues in fundamental and applied research across all scientific disciplines. However, the lack of reproducibility of early results added to the unknown, in some cases late characterization of the magnetic impurities [1] increased substantially the scepticism of the scientific community. In the year 2003 some of us reported that proton irradiation of MeV energy on HOPG samples triggers ferro- or ferrimag-

netism at room temperature [2,3]. Although reports on the reproducibility of this behavior in two different HOPG samples followed the original publication [4], the lack of independently published studies that successfully triggered magnetic order after ion irradiation of carbon pushed us to elaborate and extend our experimental work.

Although there are several theoretical works in the literature on magnetic order in carbon, specially hydrogen-induced (see for example Ref. [5] and references therein), apart from the proton induced magnetic order in graphite there are no much new systematic experimental works that show ferromagnetism in metal-free carbon, including in particular a rigorous characterization of the samples impurities. The study done in Ref. [6] reported that Nitrogen and Carbon irradiation of nanosized diamond powder triggers magnetic order at room temperature. However, no study of the impurity concentration was presented in that work. The studies done in [7] reveal that carbon films prepared by CVD on stainless steel substrates reach magnetization values of the order of 0.15 emu/g at room tem-

* Corresponding author

Email address: esquin@physik.uni-leipzig.de (P. Esquinazi).

¹ This work was supported by the DFG under grant DFG ES 86/11-1 and by the European Union under "Ferrocabon". Discussions with R. Höhne and Y. Kopelevich are gratefully acknowledged. We are in debt with D. Alber from the Hahn-Meitner-Institut in Berlin, where the NAA analysis at BER II were done, as well as with T. Agné for arranging this measurement. We thank P. Morgenstern from the Institute for Surface Modification (IOM) in Leipzig for the XRF measurements.

perature, comparable to those reported in earlier studies [8,9]. In that work the amount of measured impurities appears to be not enough to account for the absolute value of the magnetic moments of the samples. In Ref. [10] the magnetization of proton irradiated graphite was studied after one low-dose irradiation. The authors show there that proton irradiation induces Curie-type paramagnetism in graphite but no measurements of the hysteresis loops before and after irradiation were apparently done in order to check for the induced magnetic order. The experimental difficulties to reproduce this magnetic order and the weakness of the ferromagnetic signals, which are sometimes at the limit of the sensitivity of current experimental characterization methods, including SQUID's, are the main obstacles that preclude a rush development of this interesting and important subject.

The aim of this report is threefold. Firstly, we discuss the expected ferromagnetic signals after proton irradiation based on our previous publication [2] and the necessary precautions one needs to take for the SQUID measurements of these weak signals. To increase the relative sensitivity of these measurements and to avoid experimental artifacts as well as any introduction of magnetic impurities through sample handling, we developed a new, simple sample holder that allows consecutive irradiation and SQUID measurements without touching the sample or its holder as well as their relative positions. Secondly, in order to check the magnetic impurity concentration of the HOPG samples and the accuracy of the method we used (Particle Induced X-ray Emission (PIXE)), we have compared the impurity concentrations measured with three experimental methods on similar HOPG samples. Thirdly, we have irradiated three HOPG samples under different conditions and measured the changes in their magnetic behavior with a SQUID. We show that proton irradiation induces ferromagnetism in graphite, as demonstrated earlier[2], and we extend our studies to the induced paramagnetism. Through the irradiation of thousands of spots of micrometer size in a single sample we were able to measure their ferromagnetic signal and estimate the average magnetic moment of each spot.

2. Experimental details

The studies performed in Ref. [2] indicate that the ferromagnetic magnetic moment at saturation

m_s depends on the total implanted charge C_t . Roughly speaking $m_s \sim 2 \times 10^{-7} [\text{emu}/\mu\text{C}^{0.5}] C_t^{0.5}$ for $C_t < 10^3 \mu\text{C}$ (the usual magnetic moment (cgs) unit “emu” is equal to 10^{-3}Am^2). C_t means the total charge irradiated on the same area. The square root dependence suggests that at small doses the experimental signal should be directly proportional to the irradiation dose, which produces vacancies, adatom defects and/or vacancy-hydrogen complexes. However, it tends to saturate at higher doses, probably due to damage accumulation (e.g. saturation of dangling bonds), hydrogen outgassing and/or annealing of certain defects [11]. This square root relation should be taken only as a rough estimate for the expected ferromagnetic signal and for broad irradiation areas. The actual value of m_s , however, depends on parameters like proton current, i.e. the higher the current the lower is m_s , (e.g. due to heating effects), or beam size (broad or narrow beam irradiation) [4]. According to earlier results [2] we expect m_s of the order of 10^{-6} emu for a total irradiated charge of $100 \mu\text{C}$. That means that the SQUID magnetometer should provide reliable and reproducible results within a magnetic moment range better than $1 \mu\text{emu}$, specially after introducing and taking out the sample with holder several times into or from the SQUID.

Usually at fields $B \lesssim 1$ T the reproducibility of commercial SQUID's is better than $1 \mu\text{emu}$ and therefore these magnetometers can be used to measure the effects produced by irradiation (an example is shown below). Care should be taken, however, with possible artifacts of these systems, specially magnetic field hysteresis due to the electronics and/or superconducting solenoid properties [12]. The reproducibility of each SQUID system should be checked before starting the irradiation steps.

The magnetic moment measurements were performed with a SQUID magnetometer from Quantum Design with the reciprocating sample option (RSO). We note that the SQUID sensitivity without this option is not enough to measure accurately the effects produced by irradiation, specially when the magnetic signal is of the order of μemu for the saturation ferromagnetic moment. The magnetic field was applied parallel to the graphene planes in all measurements in order to diminish the diamagnetic background. As an example for the reproducibility and error, Fig. 1 shows the difference between hysteresis loops of the same HOPG sample (including holder) before irradiation measured at different days. Each measurement was performed following

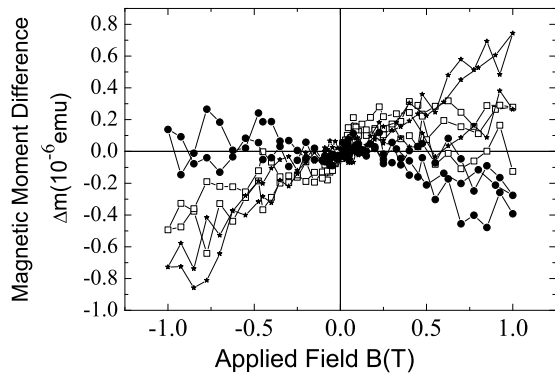


Fig. 1. Difference of magnetic moments as a function of field (hysteresis loops) measured for the same HOPG sample and holder (in this case number 3 as example) at four different days at $T = 100$ K. The difference Δm is calculated taking the measurement at a certain day as reference. Similar differences are obtained at all temperatures and choosing measurements at other days as reference.

the same sequence after removing and introducing the whole sample with holder from/into the SQUID apparatus, leaving the sample-holder several days at ambient conditions between the measurements. The difference Δm plotted in Fig. 1 should be ideally zero at all fields. We recognize, however, that both paramagnetic- as diamagnetic-like deviations are obtained after subtraction of an arbitrarily chosen hysteresis loop (measured at a certain day) from the other loops. The largest deviation obtained is of the order of 8×10^{-7} emu at a field of 1 T. Because most of the HOPG samples we have measured in their virgin states show ferromagnetic-like hysteresis loops, which origin is not related to the magnetic impurities [13], the effects produced by the irradiation are much better identified doing this point-by-point (at equal (B, T)) difference in Δm .

Because we do not know the amount of sample that remains magnetic after irradiation, all the SQUID data are presented as magnetic moment directly measured with this method. Although one knows the penetration depth of protons of the used energy in graphite ($\lesssim 48 \mu\text{m}$) it is still unclear, which is the range where the main ferromagnetic and paramagnetic signals come from. Therefore, it has little sense to divide the measured values of magnetic moment by the total sample mass. Taking into account recently done x-ray magnetic circular dichroism and magnetic force microscopy measurements of irradiated spots in 200 nm carbon films,

which provide clear evidence for the existence of magnetic order at the spot position [14], we tend to assume that the ferromagnetic layer in our samples should be mainly located at the first micrometer from the sample surface.

The irradiations were done with the high-energy nanoprobe LIPSION, a single ended 3MV SINGLETRON accelerator with a RF-source for protons and alpha particles. Two irradiation chambers allow the irradiation with proton beams of diameters as low as 50 nm up to 0.8 mm at different proton currents at MeV energy.

All three samples were HOPG from Advanced Ceramics with a rocking curve width of 0.4° (grade A).
 -(a) Sample 1 had a mass of 3.5 mg with a size $2 \times 3 \times 0.3 \text{ mm}^3$. As in Ref. [2], it was glued on a high purity Si substrate with varnish. The irradiation of this sample consisted on three broad proton spots of 2 MeV proton energy, 0.8 mm diameter each, 0.7 mm distance, 150 μC total charge per spot and a proton current of 100 nA.

-(b) Sample 2 of 5.7 mg weight and $2 \times 4 \times 0.3 \text{ mm}^3$ size was glued in the middle of a 13.5 cm long and 1 mm diameter pure Cu wire. Due to the long length and the homogeneous magnetic response of the wire, it provides a small contribution to the SQUID signal. The whole ensemble sample plus wire including the corresponding couplings for the SQUID and accelerator chamber, were used for the irradiation: first 10^4 spots and later 2×10^4 spots more. Each spot was made with a 2.25 MeV proton energy, beam diameter of $\simeq 2 \mu\text{m}$, a total charge of 1.16 nC (fluence $0.37 \text{ nC}/\mu\text{m}^2 = 2.3 \times 10^{17}$ protons/ cm^2) and we used 700 pA proton current.

-(c) Sample 3 had a mass of 10.8 mg and a size of $4 \times 3 \times 0.4 \text{ mm}^3$. It was glued with varnish on the middle of a 13.5 cm long pure quartz rod. Before fixing it a 20 nm gold film was deposited on the rod, which is necessary for the measurement of the proton current in the accelerator chamber during irradiation. For the irradiation of spots we used a $\simeq 1.5 \mu\text{m}$ diameter proton beam, which irradiated a $\simeq 5 \mu\text{m}$ diameter area following a computer controlled spiral movement. 400 spots (25 μm apart) with a total charge of 191 μC , fluence per spot of $24.3 \text{ nC}/\mu\text{m}^2$ ($1.52 \times 10^{19} \text{ cm}^{-2}$) at a proton current of 6.5 nA (10 times larger than for sample 2) and 2.25 MeV energy were prepared in sample 3.

3. Results

3.1. Impurity measurements

As described in section 1, we expect ferromagnetic-like signals of the order of a few μemu . How much ferromagnetic Fe is necessary to produce a magnetic moment of, e.g., $5 \mu\text{emu}$? From literature data one estimates easily that 23 ng pure Fe (or a volume of $\sim 3 \times 10^{-9} \text{ cm}^3$) would be enough to produce this magnetic moment assuming that this small amount is ferromagnetic at room temperature. Under these assumptions the relative Fe concentration in a typical HOPG sample would be of the order of $6 \mu\text{g/g}$. That means that we need impurity measurements that provide a sensitivity of at least $1 \mu\text{g/g}$ for Fe. The method called Particle Induced X-ray Emission (PIXE) has this sensitivity (or better) for the analysis of Fe in a carbon matrix. Our PIXE measurements performed in situ and during irradiation show that the total amount of Fe impurities in our HOPG samples is $0.6 \pm 0.04 \mu\text{g/g}$ (i.e. 0.15 ppm)[4] for grade A samples. To check the accuracy of our PIXE analysis we have measured similar HOPG samples with two other methods. Neutron Activation Analysis (NAA) on a 30 mg HOPG grade B sample with a neutron activation time of 18 days and γ -ray measuring time of 6 hours provides a total Fe impurities of $0.17 \pm 0.03 \mu\text{g/g}$. Our PIXE measurements on the same sample gave for Fe $0.17 \mu\text{g/g}$ as well. The third method used was x-ray fluorescence with a EDXRF-spectrometer Quan X. The Fe concentration in the same HOPG grade A sample measured with PIXE was below the minimum detection limit ($\sim 5 \mu\text{g/g}$) this analytical method has. The amount of other magnetic impurities was much below that for Fe (for example, $2.5 \times 10^{-3} \mu\text{g/g}$ for Co).

Concluding, assuming the worst, unlikely case, the maximum ferromagnetic magnetic moment at saturation one expects from this amount of magnetic impurities in our HOPG samples – were this amount ferromagnetic at room temperature – is $\lesssim 5 \times 10^{-7} \text{ emu}$. Certainly, one should rule out that due to an improper sample handling and between irradiation steps a small Fe grain with a mass of a few tens of ng does get fixed somewhere at the surface of the HOPG sample. Therefore, special holders as well as systematic irradiation steps are necessary.

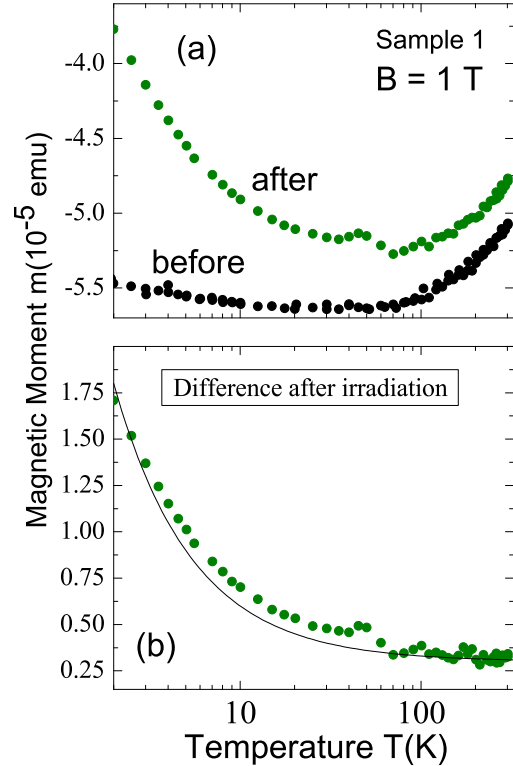


Fig. 2. (a) Total magnetic moment (HOPG sample 1 with the Si substrate) as a function of temperature at a constant magnetic field applied parallel to the graphene planes for the sample before and after proton irradiation with a broad beam (total charge $450 \mu\text{C}$ at 100 nA proton current). (b) The difference between the two curves from (a). This difference reveals directly the irradiation effect. The continuous line is the function $3 \times 10^{-5} [\text{emu K}]/T + 3 \times 10^{-6} [\text{emu}]$.

3.2. Broad irradiation

The temperature dependence of the magnetic moment before and after irradiation of sample 1 is shown in Fig. 2(a) in a semilogarithmic scale. The temperature dependence of the virgin curve shows a minimum (maximum diamagnetism) at $T \sim 30 \text{ K}$, which is usual for HOPG samples of good quality. After a broad proton beam irradiation covering most of the sample area, the magnetic moment shows a clear increase in all the temperature range. Figure 2(b) shows the difference between the magnetic moment after the irradiation minus that of the virgin state as a function of temperature at a constant field of 1 T. This difference can be roughly understood as the sum of two contributions, namely, a

paramagnetic one, which follows roughly the Curie law $3 \times 10^{-5}/T$ emu, and a ferromagnetic constant contribution 3×10^{-6} emu, i.e. $m(T, B > B_s) \simeq \frac{3 \times 10^{-5}}{T} + 3 \times 10^{-6}$, where B_s is the minimum saturation field for the ferromagnetic part. The small but clear deviation between the fit and the data shown in Fig. 2(b) can be interpreted as follows. The main variable of the Brillouin function $B_J(x)$ with $x = gJ\mu_B B/k_B T$ reaches relatively high values at low temperatures for an applied field of 1 T. Assuming for simplicity the product of the Landé factor g with the total angular momentum \vec{J} , $gJ \sim 1$, this variable is $0.13 \leq x \leq 2.2 \times 10^{-3}$ for $5 \text{ K} \leq T \leq 300 \text{ K}$ at $B = 1 \text{ T}$. Only for $x \ll 1$ one is allowed to keep the first term of the Brillouin function that provides the simple $1/T$ Curie law. Part of the deviation may also come from the assumption of a strictly temperature independent ferromagnetic contribution.

The hysteresis loops shown in Fig. 3, obtained at two temperatures subtracting the loops after irradiation from those obtained in the virgin state, justify the assumption of the two magnetic contributions. The increase of the magnetic moment after irradiation at room temperature is mainly due to the increase of the ferromagnetism of the sample; only $\sim 25\%$ of the increase is due to a paramagnetic contribution at 300 K and 1 T. The paramagnetic contribution is clearly recognized in Fig. 3 from the slope of the loops at fields above $\sim 0.25 \text{ T}$. The inset in this figure shows clearly the finite irreversibility produced by the irradiation with coercivity fields of the order of 0.02 T.

Taking into account the total irradiated charge per spot and after Ref. [2] we expect a $m_s(300) \sim 3 \times 2 \times 10^{-7} \sqrt{150} \simeq 7 \times 10^{-6}$ emu, in comparison we obtain $m_s(300) \sim 3.0 \times 10^{-6}$ emu. The results shown in Fig. 2 clearly indicate that broad irradiation – at the used proton current and fluence – triggers two magnetic contributions, one due to independent, localized magnetic moments (e.g. dangling bonds due to the disorder produced by the irradiation) and a second one with all the characteristics of magnetic order with a Curie temperature above room temperature. We stress that the effect on the magnetic properties of graphite due to proton irradiation depends on several parameters as the total implanted or irradiated charge, fluence and proton current as well as on the geometry of the used proton beam, as the next section discusses.

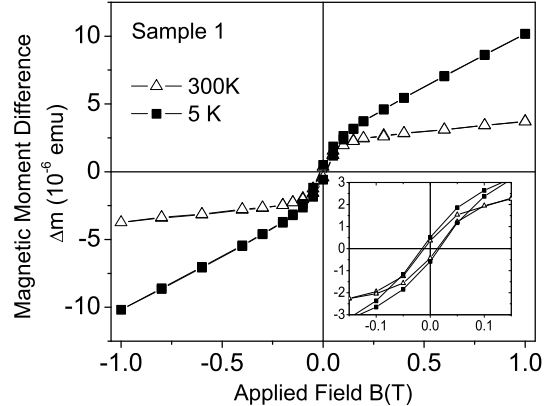


Fig. 3. Hysteresis loops for sample 1 obtained from the difference between the loops measured after and before irradiation $\Delta m = m_a - m_b$ at the same magnetic fields in each state at two temperatures. The inset blows up the data in a smaller field range.

3.3. Magnetic spots of micrometer size

3.3.1. Low proton current

Localized proton irradiation of spots of micrometer size triggers a slightly different magnetic response on graphite. Figure 4 shows the total magnetic moment (sample and holder) as a function of temperature at a field of 1 T for sample 2 in three different states, virgin, with 10^4 and with 3×10^4 irradiated spots, each of them with a total charge of 1.16 nC. The temperature dependence of m is qualitatively similar to that of Fig. 2. The difference is mainly due to the sample misalignment respect to the applied field and partially also to a different contribution of the sample holder.

The irradiation effect on the temperature dependence can be better recognized from the difference between the $m(T)$ curves shown in the inset of Fig. 4. The inset shows that no Curie-like ($1/T$)-contribution is obtained after producing the localized spots. Part of the magnetic response of the spots is due to ferromagnetism, as the hysteresis loops shown in Fig. 5 indicate. From these loops we obtain a saturation magnetic moment $m_s \sim 10^{-6}$ emu. For the first irradiation with only 10^4 spots the error involved in the subtraction, specially at low fields, does not permit to assure the existence of an hysteresis. We stress that signals of the order of 2×10^{-7} emu are at the limit of reliability (not resolution!) of our SQUID apparatus.

It is well known that the paramagnetic Curie law

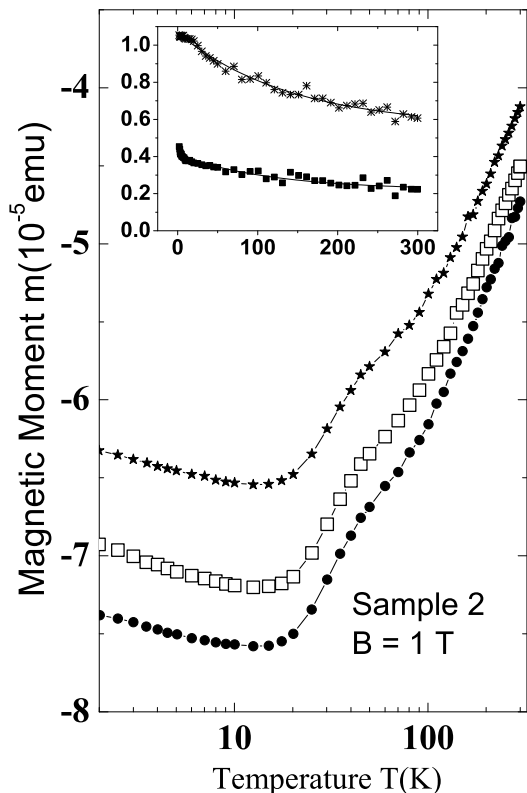


Fig. 4. Total magnetic moment of sample 2 as a function of temperature at a field of 1 T for the virgin (\bullet), after the first irradiation with 10^4 spots (total charge $11.6 \mu\text{C}$ at 700 pA (\square)), and after the second irradiation adding 2×10^4 similar spots as in the first irradiation (\star). The inset shows the difference of magnetic moment between the first (\blacksquare) (second (\star)) irradiation and the virgin state. The continuous lines are fits to the function $m_0 + m_1 \exp(-T/T_0)$ with the parameters $m_0 = 2.2(5.6) \times 10^{-6}$ emu, $m_1 = 1.9(5.07) \times 10^{-6}$ emu and $T_0 = 116(140)$ K for the first (second) irradiated sample.

holds only if $x \ll 1$. This law is a consequence of thermal average involving $(2J + 1)$ equally spaced levels, which originate from the effect of the applied field on one multiplet. If at large magnetic fields new multiplet levels start to contribute to the statistical average or if their energy levels are not equally spaced, then deviations of $m(T)$ from the Curie law to a weaker T -dependence are expected. The observed positive curvature for fields above 0.25 T in the hysteretic loops, see inset in Fig. 5, suggests that the applied field influences the number of multiplet levels that determine the total magnetic moment. The clearly weak T -dependence of the irradiated sample 2, see inset in Fig. 4, agrees with this expecta-

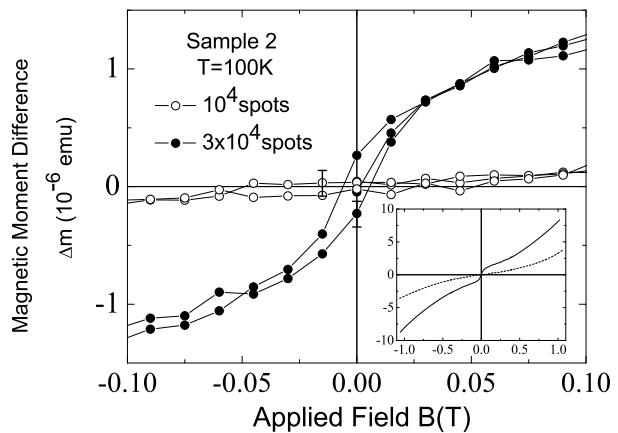


Fig. 5. Hysteresis loops for sample 2 obtained from the difference between the loops measured after and before irradiation $\Delta m = m_a - m_b$ at the same magnetic fields in the states after two irradiations at 100 K. The points (\circ) were obtained after irradiation of 10^4 spots ($11.6 \mu\text{C}$ total charge at 700 pA proton current) and (\bullet) adding 2×10^4 ($34.8 \mu\text{C}$ total charge) spots on a different area of the same sample. The bars indicate the maximum expected error due to the reproducibility of our SQUID and the subtraction. The inset shows the loops in a broader field range after the first (dashed line) and second irradiation (continuous line).

tion. The T -dependence shown in this inset can be fitted with an exponential function of the form $m \simeq m_0 + m_1 \exp(-T/T_0)$ with $m_{0,1}$ and T_0 free fitting parameters. If we use the Brillouin function plus a T -independent ferromagnetic contribution we can in principle fit the measured T -dependence but using gJ values that are above any reasonable limit, indicating its inadequacy to understand the magnetism of the irradiated spots. Whatever the reasons for the observed behavior, the measured curves indicate a constant temperature ferromagnetic-like term of the order of $m_0 \simeq 2 \times 10^{-6}$ emu for the sample with the first 10^4 spots and $m_0 \simeq 5.6 \times 10^{-6}$ emu for the sample with 3×10^4 spots at 1 T. These numbers indicate a magnetic moment of the order of 2×10^{-10} emu per spot produced at the conditions described in section 2.

3.3.2. Large proton current

From MFM (Magnetic Force Microscopy) measurements we know that higher currents decrease the magnetic phase contrast at the center of the spot, indicating the vanishing of magnetic order in part of the irradiated area [4]. To test this behavior with the

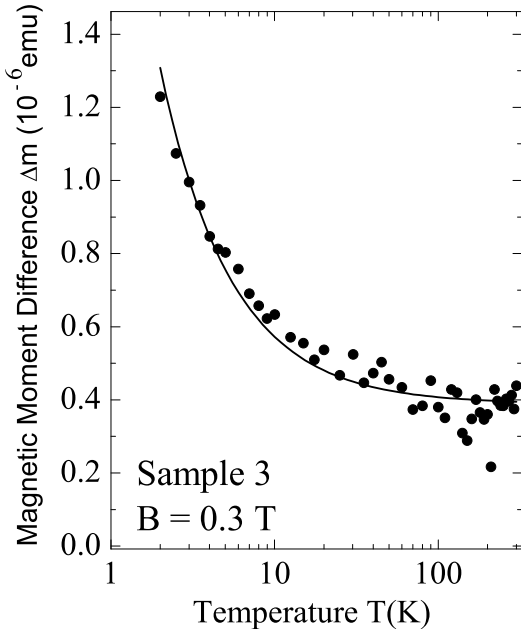


Fig. 6. Temperature dependence of the difference between the magnetic moments measured after and before the irradiation of 400 micrometer-size spots with a total charge of 191 μC at a current of 6.5 nA in sample 3. The measurements were done at a constant field of 0.3 T. The continuous line follows the equation $3.9 \times 10^{-7} [\text{emu}] + 1.84 \times 10^{-6} [\text{emu K}]/T$.

SQUID the spots in sample 3 were produced with a ~ 9 times larger proton current than for the spots produced in sample 2. Figure 6, as Fig. 2(b), shows the temperature dependence of the magnetic moment produced by the irradiation of 400 spots (fluence $24.3 \text{ nC}/\mu\text{m}^2 = 1.52 \times 10^{19} \text{ cm}^{-2}$, total charge 191 μC). In contrast to the effects of the spots produced in sample 2, the irradiation in sample 3 triggers a paramagnetic contribution that follows the Curie law plus a smaller, constant ferromagnetic-like background. This small, last contribution is recognized also in the s-shape curve at low fields obtained from the difference between the hysteresis loops. The results indicate that it is not only the total implanted charge what determines the ferromagnetic and/or the paramagnetic effect but also the proton current appears to have an important role due to overheating effects.

4. Conclusion

We have performed high sensitive measurements with a commercial SQUID with RSO option of the effects produced by proton irradiation in the MeV energy range on HOPG samples. All proton irradiations produce two magnetic contributions to the magnetic properties of HOPG. One contribution depends clearly on temperature and in some cases follows a Curie-like behavior. The second one can be attributed to ferro- or ferrimagnetism. These contributions are supported by the measured hysteresis and s-form of the loops as a function of magnetic field. The details of these contributions depend not only on the total implanted charge, the fluence but also on the proton current and the beam geometry, i.e. broad beam irradiation or localized spots. Largest ferromagnetic signals were obtained for localized spots produced at relatively low proton currents ($< 1 \text{ nA}$) and fluences $\lesssim 1 \text{ nC}/\mu\text{m}^2$ ($6.25 \times 10^{17} \text{ cm}^{-2}$). The saturation magnetic moment per micrometer spot is of the order of 10^{-10} emu . The absolute values of the observed effects are of the same order as those published in the original work of Ref. [2]. The observed decrease of the effects at large fluences and proton currents agrees with the decrease of the (magnetic) phase contrast with fluence and current observed in MFM measurements on similar spots produced in HOPG surfaces [4].

We note that both, SQUID and MFM measurements of the magnetic behavior of micrometer size spots indicate that upon irradiation conditions they may not behave ferromagnetically with a finite remanent magnetic moment at zero field. In this case the characterization of the spots by means of MFM under zero field conditions is difficult since no significant contrast difference will be measured after a change of the tip polarization or after applying a magnetic field on the spots.

Three experimental methods were used to check the amount of magnetic impurities in similar HOPG samples from the same company. The results indicate that the total amount of magnetic impurities is much below that needed to understand quantitatively the measured ferromagnetism after irradiation. With the implementation of a special sample holder for SQUID measurements and irradiation runs, we could increase the reliability of the SQUID results and rule out the influence of artifacts due to handling on the sample and its holder.

On the origin of the magnetic order in proton irra-

diated carbon we note the following. The overall results suggest that carbon defects (e.g. adatoms or vacancies) should play a role in the magnetic order observed. According to recent models [11] hydrogen at carbon defects (H-vacancy and -adatom complexes) may also contribute triggering or even enhancing a local magnetic moment. Regarding the role of hydrogen and taking into account that HOPG samples have a substantial amount of hydrogen at the first micrometer from the surface [15], one can speculate that not the implanted charge but the dissociation of molecular hydrogen (already in the sample) produced by the proton collisions may be important for the magnetic order, since in this case single hydrogen atoms may be more effective to bond at the magnetic sensitive defects.

An independent support to the SQUID and MFM results on irradiated carbon samples is provided by x-ray magnetic circular dichroism measurements on spots produced in 200 nm thick carbon films [14]. These results also suggest that it is probably not the implanted hydrogen but, *if at all*, the one already in the sample of importance.

We recommend that before selecting a particular irradiation, taking into account several of the irradiation parameters discussed in this work, the reproducibility as well as the resolution limits of the used SQUID should be checked in order to estimate the minimum irradiation and sample requirements.

References

- [1] T. Makarova, B. Sundqvist, R. Höhne, P. Esquinazi, Y. Kopelevich, P. Scharff, V. A. Davydov, L. S. Kashevarova, A. V. Rakhmanina, *Nature* 440 (2006) 707.
- [2] P. Esquinazi, D. Spemann, R. Höhne, A. Setzer, K.-H. Han, T. Butz, *Phys. Rev. Lett.* 91 (2003) 227201–1–4.
- [3] K.-H. Han, D. Spemann, P. Esquinazi, R. Höhne, V. Riede, T. Butz, *Adv. Mater.* 15 (2003) 1719–1722.
- [4] P. Esquinazi, R. Höhne, K.-H. Han, D. Spemann, A. Setzer, M. Diaconu, H. Schmidt, T. Butz, In *Carbon-Based Magnetism: an overview of the magnetism of metal-free carbon-based compounds and materials*, T. Makarova and F. Palacio (Eds.), Elsevier Science, 2006, Ch. 19, pp. 437–462.
- [5] Y. Ma, P. O. Lehtinen, A. S. Foster, R. M. Nieminen, *Phys. Rev. B* 72 (2005) 085451–1–6.
- [6] S. Talapatra, P. G. Ganesan, T. Kim, R. Vajtai, M. Huang, M. Shina, G. Ramanath, D. Srivastava, S. C. Deevi, P. M. Ajayan, *Phys. Rev. Lett.* 95 (2005) 097201–1–4.
- [7] T. Saito, T. Ozeki, K. Terashima, *Solid State Commun.* 136 (2005) 546–549.
- [8] K. Murata, H. Ushijima, H. Ueda, K. Kawaguchi, *J. Chem. Soc., Chem. Commun.* (1991) 1265–6.
- [9] K. Murata, H. Ushijima, H. Ueda, K. Kawaguchi, *J. Chem. Soc., Chem. Commun.* (1992) 567–569.
- [10] K. W. Lee, Y.-H. Lee, I.-M. Kim, C. E. Lee, *Journal of the Korean Physical Society* 47 (2005) 337–338.
- [11] P. O. Lehtinen, A. S. Foster, Y. Ma, A. Krasheninnikov, R. M. Nieminen, *Phys. Rev. Lett.* 93 (2004) 187202–1–4.
- [12] R. Höhne, P. Esquinazi, to be published.
- [13] P. Esquinazi, A. Setzer, R. Höhne, C. Semmelhack, Y. Kopelevich, D. Spemann, T. Butz, B. Kohlstrunk, M. Lösche, *Phys. Rev. B* 66 (2002) 024429–1–10.
- [14] H. Ohldag, T. Tylliszczak, R. Höhne, D. Spemann, P. Esquinazi, M. Ungureanu, T. Butz, [arXiv.org/cond-mat/0609478](https://arxiv.org/cond-mat/0609478).
- [15] P. Reichart, D. Spemann, A. Hauptner, A. Bergmaier, V. Hable, R. Hertenberger, C. Greubel, A. Setzer, T. Butz, G. Dollinger, D. Jamieson, P. Esquinazi, *Nuclear Instruments and Methods in Physics Research B* 249 (2006) 286–291.